

Review

# Advances in the Field of Graphene-Based Composites for Energy–Storage Applications

Yining Du <sup>1</sup>, Mingyang Wang <sup>1</sup>, Xiaoling Ye <sup>1</sup>, Benqing Liu <sup>1</sup>, Lei Han <sup>1</sup>, Syed Hassan Mujtaba Jafri <sup>2</sup> ,  
Wencheng Liu <sup>1,\*</sup>, Xiaoxiao Zheng <sup>1</sup>, Yafei Ning <sup>1,3</sup> and Hu Li <sup>1,3,\*</sup> 

- <sup>1</sup> Shandong Technology Centre of Nanodevices and Integration, School of Microelectronics, Shandong University, Jinan 250101, China; 202000400094@mail.sdu.edu.cn (Y.D.); mingyangwang@mail.sdu.edu.cn (M.W.); 202112357@mail.sdu.edu.cn (X.Y.); 202132396@mail.sdu.edu.cn (B.L.); lei.han@mail.sdu.edu.cn (L.H.); 202120353@mail.sdu.edu.cn (X.Z.); ningyafei@sdu.edu.cn (Y.N.)
- <sup>2</sup> Department of Electrical Engineering, Mirpur University of Science and Technology (MUST), Mirpur 10250, Pakistan; hassan.jafri@must.edu.pk
- <sup>3</sup> Shenzhen Research Institute of Shandong University, Shenzhen 518057, China
- \* Correspondence: 201912222@mail.sdu.edu.cn (W.L.); hu.li@sdu.edu.cn (H.L.)

**Abstract:** To meet the growing demand in energy, great efforts have been devoted to improving the performances of energy–storages. Graphene, a remarkable two-dimensional (2D) material, holds immense potential for improving energy–storage performance owing to its exceptional properties, such as a large-specific surface area, remarkable thermal conductivity, excellent mechanical strength, and high-electronic mobility. This review provides a comprehensive summary of recent research advancements in the application of graphene for energy–storage. Initially, the fundamental properties of graphene are introduced. Subsequently, the latest developments in graphene-based energy–storage, encompassing lithium-ion batteries, sodium-ion batteries, supercapacitors, potassium-ion batteries and aluminum-ion batteries, are summarized. Finally, the challenges associated with graphene-based energy–storage applications are discussed, and the development prospects for this field are outlined.

**Keywords:** energy–storages; graphene; lithium-ion battery; sodium-ion battery; supercapacitor



**Citation:** Du, Y.; Wang, M.; Ye, X.; Liu, B.; Han, L.; Jafri, S.H.M.; Liu, W.; Zheng, X.; Ning, Y.; Li, H. Advances in the Field of Graphene-Based Composites for Energy–Storage Applications. *Crystals* **2023**, *13*, 912. <https://doi.org/10.3390/cryst13060912>

Academic Editor: Conrad Becker

Received: 9 May 2023

Revised: 27 May 2023

Accepted: 2 June 2023

Published: 4 June 2023



**Copyright:** © 2023 by the authors. Licensee MDPI, Basel, Switzerland. This article is an open access article distributed under the terms and conditions of the Creative Commons Attribution (CC BY) license (<https://creativecommons.org/licenses/by/4.0/>).

## 1. Introduction

Exploring and utilizing renewable energy sources have become imperative in addressing the challenges of global warming and energy depletion [1]. To achieve the widespread adoption of clean and renewable energy, the development of high-performance energy–storage devices is crucial. These devices must not only effectively store energy from intermittent renewable sources but also provide a stable power supply as needed. Among various energy–storage technologies [2], graphene-based composites have gained considerable significance, despite certain limitations when compared to other carbon allotropes, such as amorphous/activated carbon and carbon nanotubes (CNT).

Graphene-based composites offer several advantages that make them attractive for energy–storage applications [3]. Graphene, a 2D material with a honeycomb-lattice structure, exhibits high-electrical conductivity, superior thermal conductivity, and a large specific surface area [4]. These properties enable efficient charge transport, effective heat dissipation, and enhanced electrochemical performance. However, it is essential to acknowledge the downsides of graphene-based composites. For instance, pristine graphene sheets tend to aggregate or restack, reducing the accessible surface area and impeding ion diffusion [5]. Overcoming this challenge involves fabricating graphene composites with suitable nanostructures or functionalizing graphene sheets to prevent restacking.

Beyond graphene, several advanced 2D materials hold promise for energy–storage devices [6]. Phosphorene [7], a monolayer of black phosphorus, offers high-charge carrier

mobility and a tunable bandgap, making it suitable for applications in lithium-ion batteries (LIBs) and supercapacitors [8,9]. Transition metal dichalcogenides (TMDs), such as molybdenum disulfide ( $\text{MoS}_2$ ) [10] and tungsten diselenide ( $\text{WSe}_2$ ) [11], exhibit unique electrochemical properties, including high capacitance and fast ion diffusion, which make them attractive for energy-storage applications. Additionally, materials like molybdenum dioxide ( $\text{MoO}_2$ ) [12] demonstrate a high-specific capacity and stability, positioning them as potential candidates for LIBs.

Despite the prospects offered by these advanced 2D materials, graphene retains several advantages for energy-storage systems [13]. Its high-electrical conductivity enables rapid charge and discharge rates, making it suitable for high-power applications. The superior thermal conductivity of graphene assists in dissipating heat generated during energy-storage processes, contributing to enhanced safety and longevity. Furthermore, graphene's large specific surface area facilitates efficient ion transport, leading to improved energy density and power density [14]. Its mechanical strength and flexibility also ensure stability and durability during charge and discharge cycles.

This review focuses on the significance of graphene-based composites in electrochemical energy-storage (EES) systems. It covers the properties and preparation methods of graphene, summarizes recent research progress on graphene-based composites for EES, discusses specific applications in electrochemical capacitors and LIBs, explores graphene-based anodes and cathodes, examines graphene-based composites for sodium-ion batteries (SIBs) and supercapacitors, and discusses graphene derivatives for EES. The review also highlights the current research trends and prospects for further improvements in the field of graphene-based composites.

## 2. The Properties and Preparation Methods of Graphene

### 2.1. Properties of Graphene

Graphene, a monolayer carbon sheet composed of  $\text{sp}^2$ -hybridized carbon atoms, has garnered extensive attention since its first isolation from graphite in 2004 [15–17]. It possesses exceptional properties due to its unique electronic structure (Figure 1). With in-plane  $\sigma$ -C-C bonds being one of the strongest in materials, graphene exhibits ultrahigh-electrical conductivity and carrier mobility of up to  $15,000 \text{ cm}^2/(\text{V s})$  at room temperature [18]. This high-electrical conductivity makes graphene an excellent candidate for improving the conductivity of graphene-based composites in energy-storage devices.

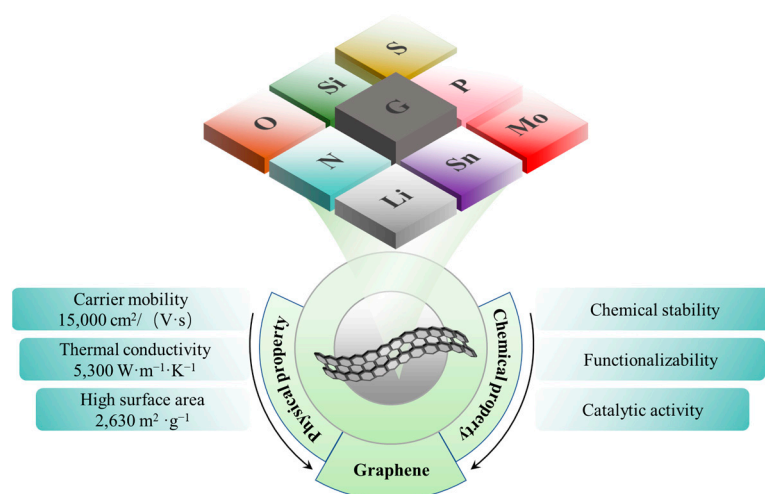


**Figure 1.** The basic properties of graphene.

The incorporation of graphene into various composites has shown remarkable improvements in energy-storage performance. For example, the combination of graphene with  $\text{MoSSe}$ , a promising anode material for LIBs, resulted in the formation of  $\text{MoSSe}/\text{graphene}$

heterostructures [19]. The introduction of graphene significantly enhanced the electrical conductivity of MoSSe, enabling a high theoretical capacity of 560.59 mAh/g. Similarly, the addition of graphene sheets to SnO<sub>2</sub> and metal organic framework (MOF) composites improved the electronic conductivity and demonstrated enhanced lithium storage performance [20].

It is important to note that the electrical conductivity of graphene is influenced by factors, such as stacking orders, the number of graphene layers, and the presence of defects [21]. Strategies, such as high-temperature treatment and doping with foreign atoms similar to N or B, have been employed to reduce defects and enhance electrical conductivity. Furthermore, graphene exhibits remarkable optical properties, with an opacity of approximately 2.3% across a wide wavelength range and a transparency of about 97% in the visible range [22]. These optical characteristics make graphene suitable for the development of transparent energy-storage devices.

In addition to its electrical and optical properties, graphene possesses exceptional thermal conductivity of up to 5300 W m<sup>-1</sup> K<sup>-1</sup> [23,24]. The incorporation of graphene into composite materials has been shown to enhance thermal conductivity, addressing the issue of uneven heat dissipation during high-current loads. For example, the addition of graphene to paraffin wax resulted in a highly thermally conductive phase change composite, exhibiting significantly increased longitudinal and transverse thermal conductivity [25].

Graphene also demonstrates excellent mechanical performance, with a greater Young's modulus (~1 TPa) and strong fracture strength [26]. These mechanical properties position graphene as a viable material for flexible and wearable energy-storage devices. Additionally, graphene's chemical inertness allows for physical adsorption interactions, such as  $\pi$ - $\pi$  stacking with other materials. Introducing defects, other atoms, and functional groups into graphene enables the fabrication of graphene with diverse properties. Furthermore, graphene's large surface area of approximately 2630 m<sup>2</sup> g<sup>-1</sup> plays a crucial role in energy-storage applications [27].

## 2.2. Mechanism of Energy-Storage and Degradation for Graphene

Graphene-based electrodes have garnered significant attention in the development of LIBs due to their unique properties and potential for improved performance [28]. The working principle of graphene-based electrodes in LIBs can be summarized as follows:

First, graphene, a 2D-carbon material with excellent electrical conductivity, allows efficient electron transport within the electrode [29]. This facilitates rapid electron movement during charging and discharging processes. Additionally, graphene's large surface area provides ample space for the attachment and intercalation of lithium ions, increasing the electrode's capacity and enabling faster ion diffusion for improved charge and discharge rates [30].

Second, graphene exhibits exceptional mechanical strength and flexibility, which ensures the stability and durability of LIBs electrodes [31]. It can withstand the volume expansion and contraction that occurs during lithium-ion intercalation and deintercalation cycles without significant structural degradation [32]. This property helps maintain electrode integrity and prolongs the battery's lifespan (Figure 2a).

However, similar to other materials, graphene is susceptible to degradation processes that occur over time. The degradation mechanisms affecting graphene include oxidation, mechanical stress, and environmental factors. In the context of LIBs, particularly those employing graphene-based electrodes, degradation refers to the gradual deterioration in performance observed over time. This degradation manifests in various ways, including reduced capacity, decreased charging and discharging efficiency, increased internal resistance, and a shortened overall battery lifespan [33]. The factors contributing to degradation in graphene-based electrodes encompass multiple aspects, such as structural changes, interactions between the electrode and electrolyte [34], the occurrence of undesirable side reactions or byproducts, and the accumulation of undesired substances, such as solid-electrolyte interphase (SEI) layers (Figure 2b). Gaining a comprehensive understanding

of these degradation processes in Li-ion batteries and implementing effective mitigation strategies are crucial to enhance their overall performance, durability, and safety in practical applications [35].

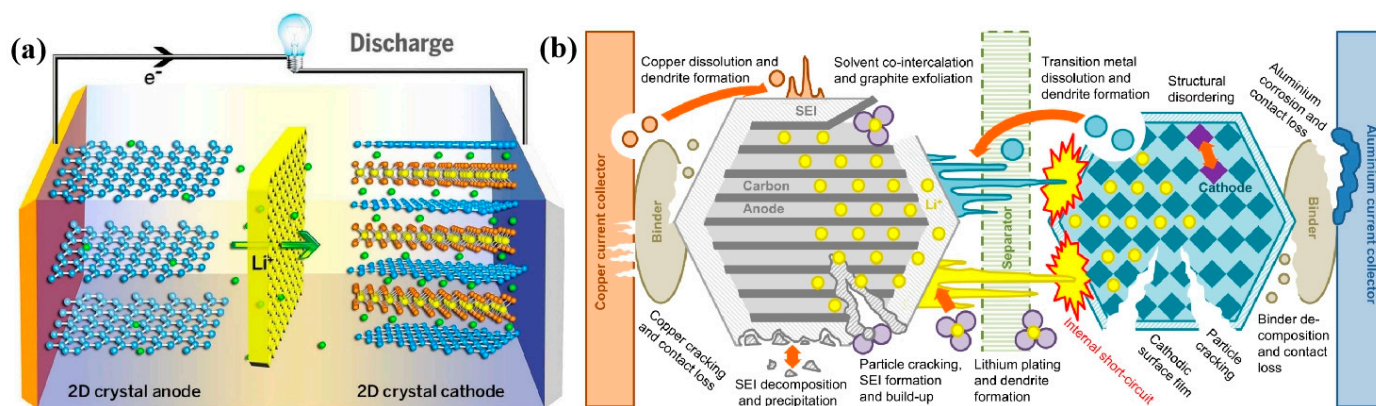


**Figure 2.** (a) Schematic of the working principle of graphene-based electrodes for LIBs. (Reproduced with permission from ref. [32]. Copyright 2022 The American Association for the Advancement of Science.) The anode is composed of graphene flakes, while the cathode comprises a hybrid graphene-Li compound, such as  $\text{LiCoO}_2$  or  $\text{LiFePO}_4$ . (b) The degradation mechanisms observed in LIBs. (Reproduced with permission from ref. [35]. Copyright 2022 Elsevier).

To mitigate degradation and ensure the long-term durability of graphene-based energy-storage devices, protective measures such as encapsulation and the application of protective coatings can be implemented [36]. Operating under controlled environmental conditions is also crucial. Furthermore, the development of graphene composites or hybrid materials can enhance the stability and longevity of graphene in energy-storage applications. These strategies contribute to the preservation of graphene's properties and the optimization of graphene-based electrodes in Li-ion batteries, promoting their reliable performance and extended lifespan [37].

### 2.3. Preparation Methods of Graphene

Graphene, a monolayer of carbon atoms arranged in a 2D honeycomb lattice, can be synthesized and fabricated using exfoliation methods [38]. Two common techniques employed are mechanical exfoliation and liquid-phase exfoliation.

Mechanical exfoliation, also known as the “Scotch tape” method, involves repeatedly cleaving bulk graphite with adhesive tape to gradually reduce the thickness until individual graphene layers are obtained [39]. This method offers the advantages of producing high-quality graphene with excellent electronic properties, allowing control over layer thickness, and being relatively low cost. However, it suffers from limitations, such as limited scalability, low yield of high-quality graphene, and lack of uniformity in the obtained flakes.

Liquid-phase exfoliation, on the other hand, disperses bulk graphite in a suitable solvent and applies mechanical forces, such as sonication, to break it down into graphene layers. This method is scalable for mass production, offers a higher yield compared to mechanical exfoliation, and allows for potential functionalization of the graphene surface [40]. However, the quality of graphene obtained through liquid-phase exfoliation is generally lower, with a higher presence of defects and impurities. Control over layer thickness is also more challenging, and additional post-processing steps may be required for purification.

In summary, mechanical exfoliation produces high-quality graphene with precise control over layer thickness but has limitations in scalability and yield [41]. Liquid-phase exfoliation allows for scalability and higher yield but compromises on the quality and control over layer thickness. Researchers continue to explore and refine these methods to overcome their limitations and unlock the full potential of graphene for various applications.

### 3. Graphene-Based Energy–Storage Systems

#### 3.1. Graphene-Based LIBs

##### 3.1.1. Mechanisms of Graphene-Based LIBs

Graphene-based electrodes have garnered significant interest in the realm of LIBs due to their unique properties, offering several advantages and presenting a potential solution for improving battery performance [42]. These advantages stem from the underlying mechanisms associated with graphene-based electrodes in LIBs [43].

One of the key mechanisms is the high-surface area of graphene. Graphene's 2D structure provides an extensive surface area, allowing for a larger number of active sites for lithium-ion adsorption and desorption during battery cycling [44]. This results in enhanced energy–storage capacity as more lithium ions can be accommodated, leading to higher battery performance.

Furthermore, the exceptional electrical conductivity of graphene facilitates rapid electron transport within the electrode material [45]. This fast electron transport enables efficient charge and discharge rates, improving the rate capability of the battery. The quick movement of electrons ensures efficient energy–storage and release, making graphene-based electrodes ideal for high-power applications.

Another mechanism is the mechanical stability of graphene [46]. Its robust structure and exceptional mechanical properties contribute to the overall stability of the electrode material. This stability helps to maintain the structural integrity of the electrode, reducing degradation and enabling a longer cycle life for the battery. Graphene's mechanical stability is crucial for achieving prolonged battery performance and durability.

By leveraging these advantages, graphene-based electrodes have the potential to significantly enhance the energy–storage capabilities, rate capability, and cycle life of LIBs [47]. However, it is important to address challenges, such as limited lithium-ion diffusion, agglomeration, restacking, scalability and cost, to fully exploit the potential of graphene-based electrodes in practical LIBs applications. Ongoing research and development efforts aim to overcome these challenges and pave the way for the widespread implementation of graphene-based electrodes in next-generation LIBs.

##### 3.1.2. Graphene-Based Anodes

Graphene-based composites have emerged as promising candidates for high-performance LIBs due to their exceptional structures and properties. Graphene serves dual roles in LIBs, acting as both a host for  $\text{Li}^+$  ions and an active material in anode composites. In 2008, Yoo et al. reported an increased lithium storage capacity by using graphene with a capacity of 540 mAh/g, compared to graphite's 372 mAh/g [48]. Incorporation of CNTs or fullerenes ( $\text{C}_{60}$ ) to graphene nanosheets further enhanced the specific capacity of LIBs, reaching up to 730 mAh/g and 784 mAh/g, respectively [49]. This highlights the importance of designing proper graphene-based composites to expand the interlayer spacing, prevent restacking, and provide additional  $\text{Li}^+$  accommodation sites to improve LIBs performance.

Various graphene-based composites have been developed by combining graphene with metal oxides, alloys, and electrochemically active nanostructures [50–52]. These composites exhibit an enhanced resistance to agglomeration during electrode preparation and cycling. The highly conductive carbon matrix formed by graphene not only improves electroconductivity but also mitigates volume changes during charge and discharge processes.

Recent research has demonstrated the potential of specific graphene-based composites in LIBs anodes. For example,  $\text{SiO}@$ graphene composites exhibited a high-reversible capacity of 1127 mAh/g at 0.2 A/g with 87% capacity retention after 200 cycles [53].  $\text{SnS-Mo}$ -graphene nanosheets composites showed a high-reversible capacity of 1128.1 mAh/g at 0.2 A/g and a capacity retention of 830 mAh/g over 600 cycles at 1.0 A/g [54]. N-doped graphene-encapsulated  $\text{MoS}_2$  nanosphere composites exhibited a reversible capacity of 975.9 mAh/g at 0.1 A/g after 100 cycles (Figure 3a–c), demonstrating excellent rate performance [55]. Additionally, rGO derivatives showed promise. An  $\text{FeS}_2/\text{rGO}$  composite exhibited a higher rate capability of 410 mAh/g at 5 C and better cyclability of

826 mAh/g after 150 cycles at 0.2 C, when compared to pure FeS<sub>2</sub>-based LIBs, as shown in Figure 3d–f [56]. A GO/black arsenic phosphorus/CNT composite exhibited stable capacities of 1286 and 339 mAh/g at current densities of 0.1 and 1 A/g, respectively, with a capacity of 693 mAh/g after 50 cycles [57]. Table 1 presents a comparison of the electrochemical properties of various representative graphene-based and derivative composites as anode electrodes in LIBs.

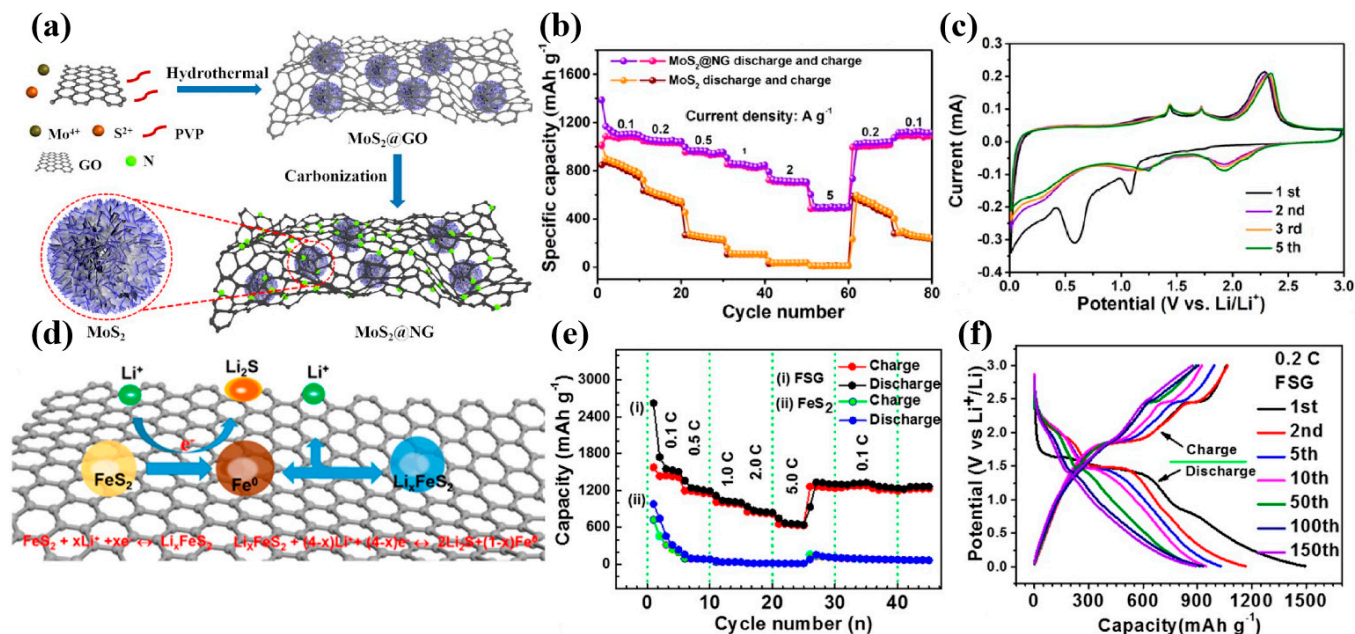


**Figure 3.** (a) The synthesis process of MoS<sub>2</sub>@NG. (b) Comparison of the rate performance between MoS<sub>2</sub> and MoS<sub>2</sub>@NG. (c) CV curves obtained at a scan rate of 0.1 mV s<sup>-1</sup>. (Reproduced with permission from ref. [55]. Copyright 2022 IOP Publishing Ltd.) (d) Schematic representation of the crystal structure conversion during the charge–discharge process of the first cycle. (e) Charge–discharge curves of FeS<sub>2</sub>-graphene composite. (f) Comparison of the charge–discharge performances between FFS<sub>2</sub>-graphene composite and FeS<sub>2</sub> at different current rates. (Reproduced with permission from ref. [56]. Copyright 2022 American Chemical Society.)

**Table 1.** Graphene-based composite as anodes for LIBs.

Composites	Specific Capacities (mAh/g)	Current Densities (A/g)	Capacity Retention (%)	Structure	References
P-doped graphene framework@porous Fe <sub>2</sub> O <sub>3</sub> nanoframework	1106	0.1	88.2	hierarchical structure	[58]
Epitaxial graphene@SiC	964.1	0.1	/		[59]
Si/SiO <sub>2</sub> @graphene	1180	2.0	91	Si/SiO <sub>2</sub> @graphene superstructure	[60]
Amorphous Fe <sub>2</sub> O <sub>3</sub> /rGO/carbon nanofibers	811	0.1	/	hierarchical structure	[61]
NiCo <sub>2</sub> S <sub>4</sub> @graphene sheets	813	0.2	85.2	mesoporous structure	[62]

Table 1. Cont.

Composites	Specific Capacities (mAh/g)	Current Densities (A/g)	Capacity Retention (%)	Structure	References
SiO <sub>2</sub> /N-doped graphene aerogel	1000	0.1	/	composite structure	[63]
Si/C particles/graphene sheet	1910.5	0.3579	/	silicon/carbon particles on graphene sheets	[64]
Carbon-coated stable Si/graphene/CNT/carbonized poly-dopamine carbon layer	1946	0.1	80.0	composite structure	[65]
Magnetite carbon nanofiber (rGO/Fe <sub>3</sub> O <sub>4</sub> CNF)	1514	0.1	/	mesoporous structure	[66]
vertical graphene sheets	105.4	5 C	/	/	[67]
D-SiO@G	774	5	/	/	[68]
2D/2D SnSe <sub>2</sub> /graphene	490.9	0.1 C	/	/	[53]

The advantages of graphene-based composites in LIBs stem from their unique properties and synergistic effects. Graphene's large surface area, high-electrical conductivity, and mechanical strength contribute to the improved Li<sup>+</sup> ion storage capacity and cycling stability [69]. Furthermore, graphene's ability to prevent restacking and enhance electron transfer promotes better charge/discharge kinetics and overall battery performance. However, challenges such as scalable and cost-effective fabrication methods, as well as potential agglomeration or degradation of graphene during cycling, need to be addressed to fully exploit the benefits of graphene-based composites [70]. The rational design of these composites, coupled with their unique properties and synergistic effects, allows for improved energy-storage capacity, enhanced cycling stability, and better rate performance. Further research efforts should focus on optimizing the structural configurations of graphene-based composites and exploring additional hybrid systems to advance LIB technology.

### 3.1.3. Graphene-Based Cathodes

By incorporating graphene into cathode materials, several benefits can be achieved, including improved electronic conductivity, enhanced specific capacities, and reduced particle agglomeration.

One example is the use of graphene in FeF<sub>3</sub> cathode materials. FeF<sub>3</sub> possesses a high-theoretical specific capacity but suffers from poor electrical conductivity and sluggish kinetics. To overcome these limitations, He et al. introduced a reduced graphene oxide (rGO) into FeF<sub>3</sub> and fabricated a flexible free-standing FeF<sub>3</sub>/chitosan pyrolytic carbon/rGO (FeF<sub>3</sub>/C/rGO) film. The incorporation of rGO not only improved the electronic conductivity but also provided a confined structure for FeF<sub>3</sub> nanoparticles, reducing the diffusion pathway for Li<sup>+</sup> ions and preventing interlayer reactions. As a result, the FeF<sub>3</sub>/C/rGO film exhibited a remarkable capacity of 220 mAh/g over 200 cycles at 100 mA/g, as shown in Figure 4a–e.

In the case of organic electrode materials, the dissolution and poor electronic conductivity pose challenges for their application in LIBs. Yang et al. addressed these issues by developing a cathode nanocomposite composed of anthraquinone carboxylate lithium salt (LiAQC) and graphene (nr-LiAQC/G) [71]. The introduction of graphene improved the electronic conductivity of the composite, while the nanorod structure of LiAQC shortened the transport distance between Li<sup>+</sup> ions and electrons. Moreover, the hydrophilic -CO<sub>2</sub>Li groups on the LiAQC surface reduced its dissolution in the electrolyte. These synergistic effects resulted in a high-initial discharge capacity of 187 mAh/g at 0.1 C, good cycling stability with a reversible capacity of approximately 165 mAh/g after 200 cycles at 0.1 C, and excellent rate capability (Figure 4f–h).

The modification of cathode materials using graphene can also be seen in  $V_6O_{13}$  and  $V_2O_5$  systems. Wu et al. employed rGO to modify  $V_6O_{13}$ , leading to an improved electrical conductivity and stability [72]. The resulting  $V_6O_{13}$ @rGO composite exhibited enhanced electrical performance, compared to pristine  $V_6O_{13}$ . Similarly, Chen et al. blended graphene with  $V_2O_5$  to enhance its electronic conductivity [73]. The  $V_2O_5$ @G composite demonstrated a high-discharge capacity of 313.65 mAh/g at 150 mA/g, excellent cycling stability, and good rate capability. Some other graphene-based composites, as cathodes for LIBs, have been summarized in Table 2.

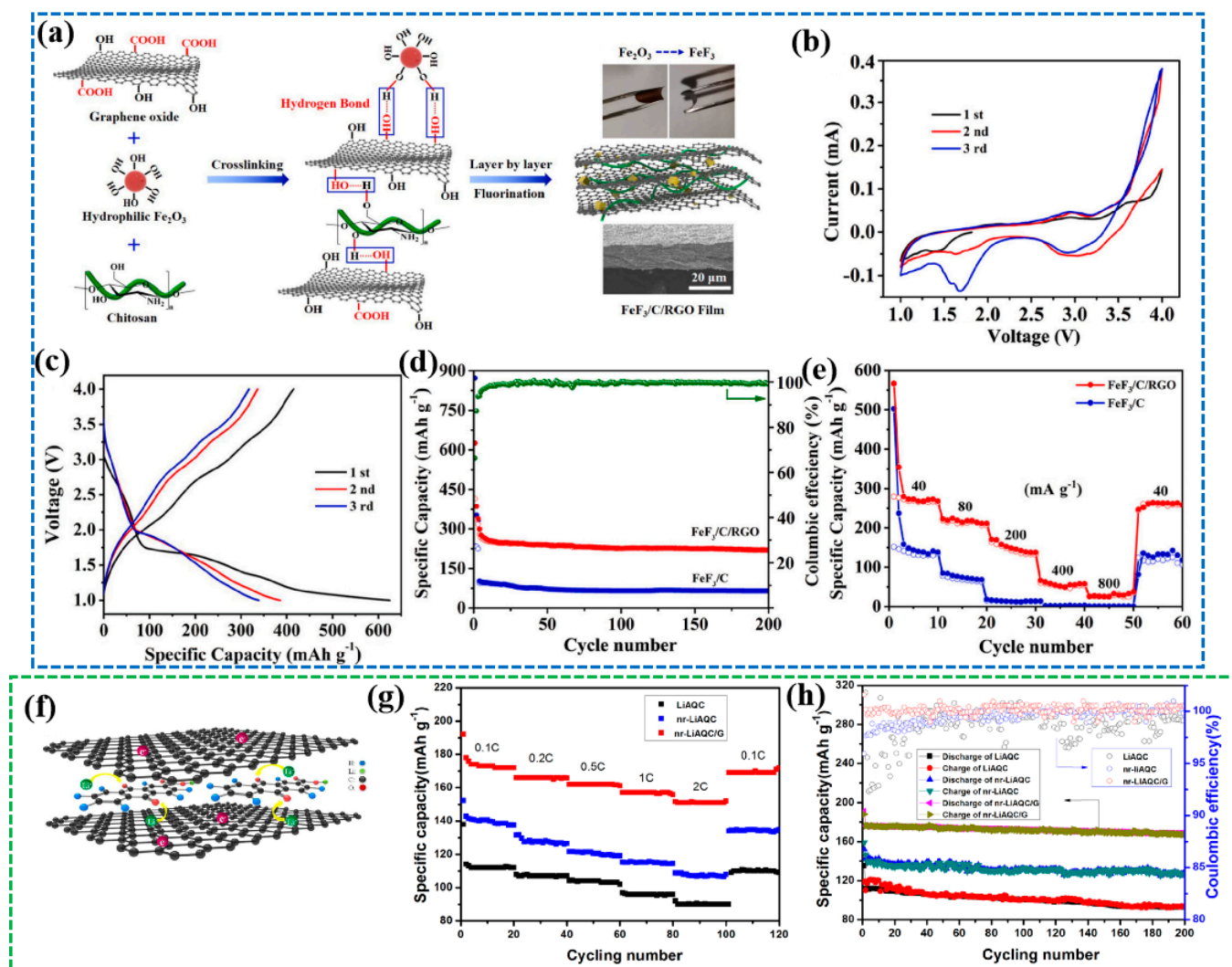


**Figure 4.** (a) Schematic illustration depicting the synthetic procedure of the  $FeF_3/C/RGO$  film. (b) CV curves obtained from the  $FeF_3/C/RGO$  film. (c) Charge/discharge profiles observed for the  $FeF_3/C/RGO$  film. (d) Cycling performance analysis of the  $FeF_3/C/RGO$  film. (e) Rate performance evaluation of the  $FeF_3/C/RGO$  film and  $FeF_3/C$  powder at a current density of 100 mA  $g^{-1}$ . (Reproduced with permission from ref. [74]. Copyright 2022 Elsevier B.V.). (f) Schematic representation of the lithium ion insertion process in nr-LiAQC/G. (g) Cycling performance comparison among LiAQC, nr-LiAQC, and nr-LiAQC/G. (h) Rate capabilities analysis of LiAQC, nr-LiAQC, and nr-LiAQC/G. (Reproduced with permission from ref. [71]. Copyright 2022 American Chemical Society).

**Table 2.** Graphene-based composite as cathodes for LIBs.

Composites	Specific Capacities (mAh/g)	Current Densities	References
Cellulose nanofiber derived carbon and rGO co-supported LiFePO <sub>4</sub> nanocomposite	168.9	0.1 C	[75]
VO <sub>2</sub> (B)/rGO	226.0	0.05 A/g	[76]
LiFePO <sub>4</sub> /graphene nanoplatelets	153.0	0.1 C	[77]
FePO <sub>4</sub> -GO	145.0	0.5 C	[78]
Core double-shell Ti-doped LiMnPO <sub>4</sub> @NaTi <sub>2</sub> (PO <sub>4</sub> ) <sub>3</sub> @C/3D graphene	164.8	0.05 C	[79]
Li <sub>1.2</sub> Mn <sub>0.6</sub> Ni <sub>0.2</sub> O <sub>2</sub> -N-doped graphene carbon matrix	286.4	0.2 C	[80]
3D holey graphene wrapped Li <sub>3</sub> V <sub>2</sub> (PO <sub>4</sub> ) <sub>3</sub> /N-doped carbon	78.0	150 C	[81]
MoS <sub>2</sub> /rGO	900.0	5 C	[82]
spheres of graphene and carbon nanotubes	547	5	[83]
dual-porous COF, USTB-6	188	10 C	[84]
VO <sub>2</sub> (B)/rGO	226	50 m	[73]
LiNi <sub>0.5</sub> Mn <sub>1.5</sub> O <sub>4</sub>	132.4	0.1 C	[85]
V <sub>2</sub> O <sub>5</sub> ·nH <sub>2</sub> O/reduced graphene oxide	196	1	[86]

While graphene integration offers several advantages, it is important to consider some limitations as well. One potential drawback is the cost associated with the large-scale production of high-quality graphene. Additionally, the dispersibility of graphene in the cathode matrix and its interaction with other components needs careful optimization to achieve optimal performance. The incorporation of graphene into cathode materials for LIBs provides numerous benefits, including improved electronic conductivity, enhanced specific capacities, and reduced particle agglomeration. By addressing the limitations of conventional cathode materials, graphene-based composites have shown impressive electrochemical performances. However, further research is required to optimize the graphene-cathode interface, overcome scalability challenges, and explore the full potential of graphene-based cathode materials in LIBs.

### 3.2. Graphene-Based SIBs

SIBs have garnered widespread attention as a low-cost alternative to LIBs. This is primarily due to the abundance and cost-effectiveness of sodium, as well as its redox potential, which is only 0.3 V higher than that of lithium [87]. The working mechanism of SIBs involves the migration of Na<sup>+</sup> ions in the electrolyte between the anode and cathode, while the electrons are transmitted through the outer circuit, similar to LIBs.

Numerous studies have focused on the development of high-performance SIBs, with a key focus on exploring suitable electrode materials. Graphene has emerged as a promising material for SIBs fabrication due to its unique structure and surface-mediated ion storage process. For instance, Liu et al. employed a pore-forming technique to create nanopores in graphene, facilitating the in situ growth of Co<sub>3</sub>Se<sub>4</sub> nanoparticles on defective graphene [88]. The nanopores broke through the physical barrier of graphene nanosheets, enabling rapid longitudinal diffusion of electrolyte ions. The resulting Co<sub>3</sub>Se<sub>4</sub>/holey graphene composite, used as an anode material for SIBs, exhibited remarkable rate performance of 519.5 mAh/g at 5.0 A/g and satisfactory cycle stability. These excellent properties can be attributed to the high conductivity and fast ion transport facilitated by the ingenious structure.

Another notable material for SIBs anodes is the Sb/rGO (antimony/reduced graphene oxide) composite. Amardeep et al. prepared this composite through a simple route, as

shown in Figure 5a–c [89]. The Sb/rGO composite demonstrated a high-reversible Na-storage capacity of approximately 550 mAh/g (at 0.2 A/g) and a first-cycle Coulombic efficiency of nearly 79% as an SIBs anode. This excellent reversibility was attributed to the coarse particle size of Sb and the encapsulation of rGO within the Sb particles. Furthermore, the Sb/rGO-based electrode exhibited good cyclic stability with negligible capacity fade after 150 cycles (approximately 97% capacity retention). It also demonstrated high-rate capability with over 86% capacity achieved when the current density was increased from 0.1 to 2 A/g, resulting in a capability of nearly 490 mAh/g even at 2 A/g.

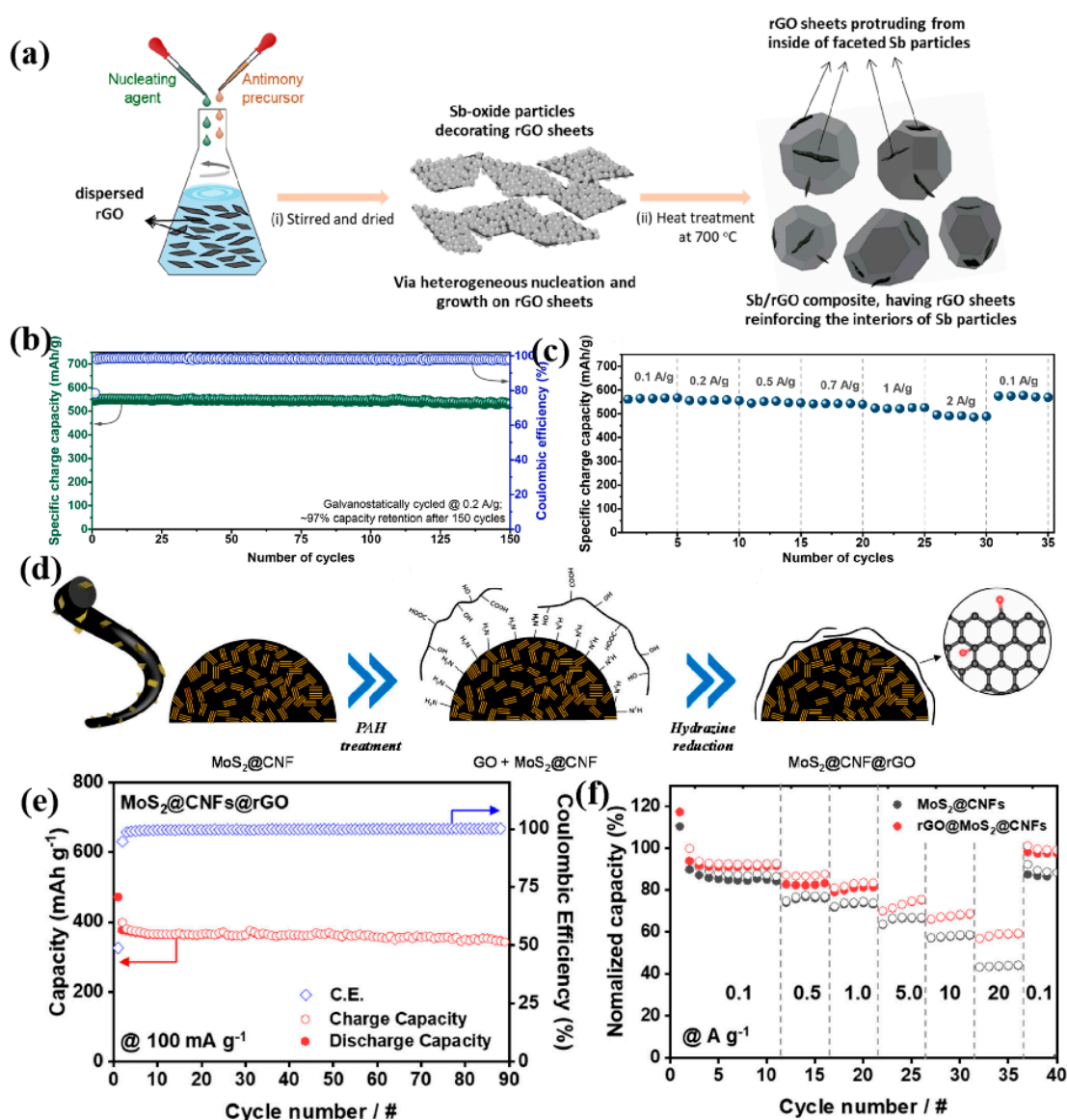


**Figure 5.** (a) Schematic illustration depicting the synthetic procedure of Sb/rGO composite. (b) Variations in reversible Na-storage capacities with current densities during continuous galvanostatic cycling runs. (c) Variations in specific Na-storage capacities and Coulombic efficiencies of the developed Sb/rGO composite at a current density of 0.2 A/g in Na “half” cells. (Reproduced with permission from ref. [89]. Copyright 2022 American Chemical Society). (d) Schematic illustration illustrating the preparation process of MoS<sub>2</sub>@CNFs@rGO. (e) Cycling performance analysis at a current density of 100 mA g<sup>-1</sup>. (f) Rate capability analysis with different current densities (0.1 A g<sup>-1</sup>~20 A g<sup>-1</sup>). (Reproduced with permission from ref. [90]. Copyright 2022 Multidisciplinary Digital Publishing Institute).

MoS<sub>2</sub>, with its 2D layered structure suitable for stable insertion of sodium ions, is another promising material for SIBs anodes. However, its practical application is limited by intrinsic issues, such as low electronic conductivity and loss of sulfur (S) elements during conversion reactions. To address these challenges, Cho et al. prepared interlayer-enlarged MoS<sub>2</sub> nanoflakes doubly covered with carbon nanofibers (CNFs) and rGO (MoS<sub>2</sub>@CNFs@rGO) [90]. The addition of CNFs and rGO improved the electronic conductivity of the composite and prevented the loss of S during repetitive conversion reactions (Figure 5d–f). The synergistic effect of these three components enabled the MoS<sub>2</sub>@CNFs@rGO-based anode to exhibit a high capacity of 345.8 mAh/g at a current density of 100 mA/g for 90 cycles.

In addition to its use in anode materials, graphene also holds great potential for enhancing the performance of traditional cathode materials in SIBs. For example, Na<sub>2</sub>MnP<sub>2</sub>O<sub>7</sub>, a non-toxic, low-cost, and high-potential cathode candidate, shows promise for advanced SIBs. However, its practical application is hindered by a poor high-rate performance, low-initial Coulombic efficiency, and unsatisfactory cycling ability, mainly due to low-electronic conductivity and manganese dissolution.

To overcome these challenges, Li et al. utilized graphene to modify Na<sub>2</sub>MnP<sub>2</sub>O<sub>7</sub> through a facile high-energy vibrating activation process, resulting in NMP@GL [91]. The obtained NMP@GL cathode exhibited an ultrahigh-initial Coulombic efficiency of 90% and a high-energy density exceeding 300 Wh/kg. Additionally, the rate performance and cycling stability were significantly improved with a capacity retention of 83% after 600 cycles at 2 C. These improvements can be attributed to the addition of graphene, which accelerated electron transport and suppressed manganese dissolution.

It is worth noting that further research and optimization are still required to address the challenges associated with SIBs, including electrode material selection, scalability, and long-term stability [5]. Nonetheless, the progress achieved so far underscores the potential of SIBs as a viable alternative in the field of energy–storage.

### 3.3. Graphene-Based Supercapacitors

As an important energy–storage device, supercapacitors have garnered significant attention due to their ability to store electrochemical energy through mechanisms such as electric double layer capacitance (EDLC) and pseudocapacitance [91]. EDLC stores energy by reversible electrostatic adsorption of electrolyte ions on the active material, and achieving high capacitance relies on electrodes with large specific surface areas and high conductivity [92]. Graphene and its derivatives have been extensively studied for their excellent electrical properties, large specific surface area, and unique mechanical properties [93]. The intrinsic capacitance of monolayer graphene has been reported to be approximately 21 mF/cm<sup>2</sup>, yielding a theoretical capacitance of nearly 550 F/g when utilizing the entire graphene surface area.

However, the practical capacitance values obtained thus far are significantly lower than the theoretical values, primarily due to the strong  $\pi$ – $\pi$  interactions between individual graphene sheets leading to aggregation. This aggregation phenomenon reduces the pristine specific surface area of graphene and consequently lowers its capacitance. To mitigate aggregation, various strategies have been explored, including the introduction of other species such as CNTs, carbon spheres, and non-carbon nanoparticles. For instance, Wang et al. employed a simple, green, hydrothermal route to introduce CNTs into graphene [94]. This approach regulated the stacking of graphene sheets and maintained spacing between adjacent sheets, thereby enhancing the effective surface area and supercapacitor performance of the composite. The resulting supercapacitor exhibited a high-specific capacitance of 318 F/g and an energy density of 11.1 (W h)/kg.

Apart from the introduction of other species, the surface chemistry of graphene also plays a crucial role in determining its capacitive performance. Sun et al. utilized p-phenylenediamine and ammonia as reduction and doping agents, respectively, to prepare nitrogen-doped porous 3D graphene via a mild one-pot hydrothermal process [95]. By

varying the doping content, they achieved different nitrogen concentrations (6.52–7.81%) in the 3D graphene samples, which regulated the capacitive behavior. The highest specific capacitance in their study reached 788 F/g at a current density of 0.5 A/g, with 296 F/g at 10 A/g, as shown in Figure 6a–c. Arvas et al. reported a novel method, known as Yucel’s method, for fabricating nitrogen-based graphene electrodes with high-performance supercapacitors [96]. By controlling the applied potential range, different functional groups formed on the graphene, and the specific capacitance ranged from 178 mF/cm<sup>2</sup> to 2034 mF/cm<sup>2</sup> at a current density of 10 mA/cm<sup>2</sup>.

Despite the significant improvements achieved through the aforementioned methods, the energy density and cyclic stability of graphene-based supercapacitors still fall short of practical requirements [97]. Therefore, it is necessary to incorporate additional materials, such as pseudocapacitive materials, to enhance the energy density. He et al. developed a 3D porous phosphotungstic acid/rGO composite through a one-pot hydrothermal process [98]. Phosphotungstic acid molecules were uniformly anchored on the surface of rGO sheets via electrostatic interactions, preventing aggregation of rGO. Additionally, phosphotungstic acid exhibited fast reversible multi-electron redox reactions, contributing to pseudocapacitance [99]. The resulting phosphotungstic acid/rGO composite demonstrated a high-specific capacitance of 456.7 F/g at 5 mV/s and 363.8 F/g at 0.5 A/g, surpassing the capacitance values obtained from rGO alone (162.4 F/g at 5 mV/s and 190.6 F/g at 0.5 A/g) (Figure 6d–f). Moreover, the phosphotungstic acid/rGO composite exhibited good cyclic stability, retaining 82.9% of its initial capacitance after 1000 charge–discharge cycles. Table 3 provides a summary and comparison of the electrochemical performances of various supercapacitors based on graphene-based composites. Strategies, such as doping with other atoms, chemical modification, and hybridization of graphene with other active materials, have significantly improved the practical capacitance of graphene-based supercapacitors. However, further efforts are required to achieve higher capacitance and broaden the practical applications of graphene-based supercapacitors.

**Table 3.** Comparison of electrochemical performances of graphene-based composite electrodes for supercapacitor.

Composites	Capacities (F/g)	Condition	References
Al-doped Co <sub>9</sub> S <sub>8</sub> @N-doped graphene	134.00	Aqueous KOH electrolyte, 1 A/g	[100]
rGO/KCu <sub>7</sub> S <sub>4</sub>	815.83	6M PVA/KOH, 0.5 A/g	[101]
Anthraquinone-based covalent organic frameworks/graphene composite aerogel	378.0	1 M H <sub>2</sub> SO <sub>4</sub> aqueous electrolyte, 1 A/g	[60]
W <sub>18</sub> O <sub>49</sub> nanowires-rGO	365.5	AlCl <sub>3</sub> aqueous electrolyte, 1 A/g	[102]
(Ni, Mo)S <sub>2</sub> /graphene	2379.0	Aqueous KOH electrolyte, 1 A/g	[23]
CoWO <sub>4</sub> -CoMn <sub>2</sub> O <sub>4</sub> /N-doped graphene	4133.3	Aqueous KOH electrolyte, 2 A/g	[103]
Graphene/VO <sub>x</sub>	1110.0	LiCl electrolyte	[104]
Ti <sub>3</sub> C <sub>2</sub> T <sub>x</sub> /graphene/Ni	542.0	1 M H <sub>2</sub> SO <sub>4</sub> electrolyte, 5 mV/s	[105]
Perovskite material (La <sub>0.8</sub> Sr <sub>0.2</sub> Mn <sub>0.5</sub> Co <sub>0.5</sub> O <sub>3-δ</sub> . LSMCO)	55.0	5 mV/s	[106]
rGO/Cu-MOF@PANI	5	276.0 A/g	[107]
Ag/RGO/CF	350 ± 9	5 mV/s	[108]
Single- and Multi-Layer Graphene/Mn <sub>3</sub> O <sub>4</sub>	452	1 mV/s	[109]

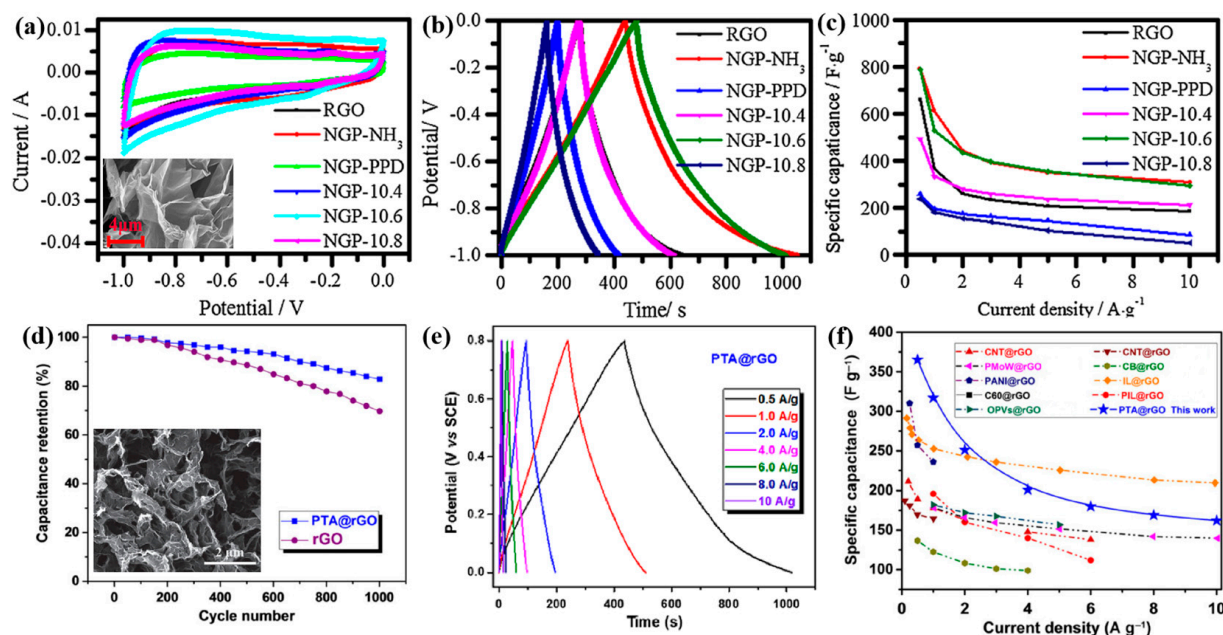


**Figure 6.** (a) CV curves, (b) charge/discharge curves and (c) specific capacitances obtained from the supercapacitor performances of the as-prepared samples. (Reproduced with permission from ref. [95]. Copyright 2018 Springer Nature). (d) Capacitance retentions comparison between rGO and PTA@rGO electrodes. (e) Charge/discharge curves of PTA@rGO at various current densities. (f) Specific capacitances of the PTA@rGO electrode as a function of current densities, along with a comparison to other reported references. (Reproduced with permission from ref. [99]. Copyright 2018 John Wiley and Sons).

### 3.4. Graphene-Based Composites for EES beyond LIBs, SIBs and Supercapacitors

#### 3.4.1. Potassium-Ion Batteries

Graphene-based, potassium-ion batteries (PIBs) have emerged as a highly promising energy-storage solution, attracting significant interest in recent years [44]. This section provides a comprehensive overview of PIBs, encompassing their working mechanism, advantages and disadvantages, and the latest research advancements.

In PIBs, graphene-based materials serve as crucial electrode materials. During the charging process, potassium ions ( $K^+$ ) undergo intercalation into the graphene structure, accompanied by the insertion or adsorption of counter ions (e.g.,  $PF_6^-$ ) from the electrolyte. This mechanism is commonly referred to as the intercalation or adsorption mechanism. The intercalation/adsorption of  $K^+$  ions within the graphene layers induces changes in the electronic structure of graphene, enabling the storage and release of electrical energy [110].

Considerable progress has been achieved in the development of graphene-based PIBs, driven by extensive research efforts. Researchers have explored various strategies to enhance the electrochemical performance of PIBs [111]. Notably, the incorporation of graphene with other active materials, such as metal oxides, metal sulfides, and carbon-based materials, has demonstrated promising outcomes. These composite electrodes exhibit improved specific capacity, enhanced rate capability, and exceptional cycling stability.

Furthermore, significant attention has been devoted to surface functionalization and interfacial engineering techniques for tailoring the properties of graphene-based electrodes. The introduction of heteroatoms into graphene structures has been explored as a means to modify the charge storage mechanisms and enhance the overall performance of PIBs [18]. Additionally, substantial efforts have been made to deepen the understanding of the fundamental electrochemical processes and mechanisms underlying PIBs, facilitating the rational design of graphene-based electrode materials.

### 3.4.2. Aluminum-Ion Batteries

Graphene-based aluminum-ion batteries (AIBs) have emerged as a promising energy-storage technology, offering potential advantages in terms of high-energy density, fast charging capability, and improved safety [112]. In AIBs, graphene-based materials are utilized as electrode materials. During the charging process, aluminum ions ( $\text{Al}^{3+}$ ) are intercalated into the graphene structure, accompanied by the reversible extraction and insertion of anions (e.g.,  $\text{Cl}^-$ ,  $\text{SO}_4^{2-}$ ) from the electrolyte. This intercalation/deintercalation process occurs through the migration of  $\text{Al}^{3+}$  ions between the cathode and anode, resulting in the storage and release of electrical energy [113]. The structural properties of graphene, including its large surface area, high-electrical conductivity, and mechanical flexibility, facilitate the intercalation/deintercalation process.

Recent research efforts have been focused on addressing the challenges associated with graphene-based AIBs and exploring new avenues for improvement [114]. Strategies, such as nanostructuring the graphene materials, designing advanced electrolyte systems, and incorporating nanoscale additives, have been investigated to enhance the electrochemical performance of AIBs. By nanostructuring the graphene materials, researchers aim to increase the surface area and expose more active sites for efficient ion intercalation. The design of advanced electrolyte systems plays a crucial role in optimizing the ionic conductivity and stability of AIBs [115]. Additionally, the incorporation of nanoscale additives can improve the structural stability and enhance the overall performance of AIBs.

Furthermore, the development of advanced characterization techniques and theoretical modeling approaches has provided valuable insights into the fundamental processes and mechanisms governing AIBs [116]. These insights have contributed to the rational design of graphene-based electrode materials with improved electrochemical properties. Researchers have used advanced characterization techniques, such as in situ spectroscopy and microscopy, to study the structural and electrochemical behavior of AIBs during operation. Theoretical modeling approaches, including density functional theory calculations and molecular dynamics simulations, have been employed to gain a deeper understanding of the intercalation/deintercalation process and guide the design of electrode materials with enhanced performance.

## 4. Conclusions and Perspective

In this review, we have provided an overview of the recent advancements in graphene-based, energy-storage devices, focusing on their applications in LIBs, SIBs, supercapacitors, PIBs and AIBs. The remarkable properties of graphene, such as its ultrahigh-electronic conductivity and large surface area, make it highly suitable for the fabrication of high-performance electrode materials. The incorporation of graphene and its derivatives into traditional energy-storage materials has resulted in significant improvements in device performance, attributed to the synergistic effects achieved.

While graphene-based composites demonstrate great potential for energy-storage devices, several challenges need to be addressed before their practical application in various fields. Firstly, it is crucial to explore more efficient strategies for the mass production of high-quality graphene and its derivatives, as this is essential for expanding the applications of graphene in energy-storage devices. Secondly, despite numerous reports on graphene-based composites with improved electrochemical performances, the precise working mechanisms and molecular interactions between each component remain unclear. Further investigations are necessary to elucidate these aspects. Thirdly, optimization of the graphene-to-other active material ratios and the development of multifunctional morphologies are necessary to further enhance the performance of energy-storage devices.

In conclusion, graphene-based composites have undeniably facilitated the development of high-performance energy-storage devices. To achieve practical applications of graphene-based, energy-storage devices, more efforts need to be dedicated to addressing the existing challenges through theoretical calculations and experimental research. It

is anticipated that significant breakthroughs will be made in the coming years, further advancing the practical implementation of graphene-based, energy-storage devices.

Looking forward, there are several areas that hold promise for further improvement and advancement of graphene-based composite materials in the field of energy-storage.

Firstly, exploring novel synthesis methods that enable the production of graphene-based composites with enhanced structural and morphological control will be crucial. This includes investigating techniques for fabricating hierarchical structures, tailored porosity, and controlled interfacial properties. Such advancements would allow for the precise tuning of material properties, leading to improved energy-storage performance.

Secondly, gaining a deeper understanding of the fundamental mechanisms and molecular interactions within graphene-based composites is essential for their continued improvement. Future research should focus on comprehensive characterizations and theoretical investigations to unravel the underlying working principles and optimize the design of graphene-based, energy-storage devices.

Thirdly, the integration of graphene with other emerging materials, such as metal oxides, metal sulfides, and carbon-based nanomaterials, presents exciting opportunities. The combination of these materials can potentially enhance the electrochemical performance, stability, and energy-storage capabilities of graphene-based composites. Exploring new hybrid architectures and exploring synergistic effects between different materials will be key in unlocking their full potential.

Additionally, the development of scalable and cost-effective manufacturing processes for graphene-based composites is of the utmost importance. Mass production techniques that maintain the quality and integrity of graphene while achieving large-scale production will be instrumental in realizing the practical applications of these materials in energy-storage devices.

In summary, the prospects for further improving and advancing graphene-based composite materials in the field of energy-storage are promising. Through continued research and development efforts, addressing key challenges and exploring new opportunities, graphene-based composites have the potential to revolutionize energy-storage technologies and enable the practical implementation of high-performance energy-storage devices in various applications.

**Author Contributions:** Conceptualization, W.L. and H.L.; methodology, Y.D. and M.W.; investigation, X.Y. and B.L.; data curation, L.H., Y.N. and B.L.; writing—original draft preparation, X.Y., Y.D., M.W. and X.Z.; writing—review and editing, S.H.M.J.; visualization, W.L. and X.Z.; funding acquisition, H.L. All authors have read and agreed to the published version of the manuscript.

**Funding:** This work is supported by Shandong Provincial Natural Science Foundation (Grant No.: ZR2022ZD05 and ZR2021QE148), Shandong Provincial Natural Science Foundation for Excellent Young Scientists Fund Program (Overseas) (Grant No.: 2022HWYQ-060), and Guangdong Basic and Applied Basic Research Foundation (Grant No.: 2022A1515011473 and 2023A1515011218).

**Institutional Review Board Statement:** Not applicable.

**Informed Consent Statement:** Not applicable.

**Data Availability Statement:** No new data were created or analyzed in this study. Data sharing is not applicable to this article.

**Conflicts of Interest:** The authors declare no conflict of interest.

## References

1. Fleischmann, S.; Mitchell, J.B.; Wang, R.; Zhan, C.; Jiang, D.-E.; Presser, V.; Augustyn, V. Pseudocapacitance: From fundamental understanding to high power energy storage materials. *Chem. Rev.* **2020**, *120*, 6738–6782. [[CrossRef](#)] [[PubMed](#)]
2. Chen, K.; Wang, Q.; Niu, Z.; Chen, J. Graphene-based materials for flexible energy storage devices. *J. Energy Chem.* **2018**, *27*, 12–24. [[CrossRef](#)]
3. Samorì, P.; Kinloch, I.; Feng, X.; Palermo, V. Graphene-based nanocomposites for structural and functional applications: Using 2-dimensional materials in a 3-dimensional world. *2D Mater.* **2015**, *2*, 030205. [[CrossRef](#)]

4. Yang, T.; Xia, J.; Piao, Z.; Yang, L.; Zhang, S.; Xing, Y.; Zhou, G. Graphene-based materials for flexible lithium–sulfur batteries. *ACS Nano* **2021**, *15*, 13901–13923. [[CrossRef](#)]
5. Zhang, Y.; Xia, X.; Liu, B.; Deng, S.; Xie, D.; Liu, Q.; Wang, Y.; Wu, J.; Wang, X.; Tu, J. Multiscale graphene-based materials for applications in sodium ion batteries. *Adv. Energy Mater.* **2019**, *9*, 1803342. [[CrossRef](#)]
6. Zhang, X.; Hou, L.; Ciesielski, A.; Samori, P. 2D materials beyond graphene for high-performance energy storage applications. *Adv. Energy Mater.* **2016**, *6*, 1600671. [[CrossRef](#)]
7. Rabiei Baboukani, A.; Khakpour, I.; Drozd, V.; Wang, C. Liquid-Based Exfoliation of Black Phosphorus into Phosphorene and Its Application for Energy Storage Devices. *Small Struct.* **2021**, *2*, 2000148. [[CrossRef](#)]
8. Jain, R.; Narayan, R.; Sasikala, S.P.; Lee, K.E.; Jung, H.J.; Kim, S.O. Phosphorene for energy and catalytic application—Filling the gap between graphene and 2D metal chalcogenides. *2D Mater.* **2017**, *4*, 042006. [[CrossRef](#)]
9. Pang, J.; Bachmatiuk, A.; Yin, Y.; Trzebicka, B.; Zhao, L.; Fu, L.; Mendes, R.G.; Gemming, T.; Liu, Z.; Rummeli, M.H. Applications of phosphorene and black phosphorus in energy conversion and storage devices. *Adv. Energy Mater.* **2018**, *8*, 1702093. [[CrossRef](#)]
10. Garcia-Dali, S.; Paredes, J.I.; Munuera, J.M.; Villar-Rodil, S.; Adawy, A.; Martinez-Alonso, A.; Tascón, J.M. Aqueous cathodic exfoliation strategy toward solution-processable and phase-preserved MoS<sub>2</sub> nanosheets for energy storage and catalytic applications. *ACS Appl. Mater. Interfaces* **2019**, *11*, 36991–37003. [[CrossRef](#)]
11. Muska, M.; Yang, J.; Sun, Y.; Wang, J.; Wang, Y.; Yang, Q. CoSe<sub>2</sub> nanoparticles dispersed in WSe<sub>2</sub> nanosheets for efficient electrocatalysis and supercapacitance applications. *ACS Appl. Nano Mater.* **2021**, *4*, 5796–5807. [[CrossRef](#)]
12. Han, D.; Hwang, S.; Bak, S.-M.; Nam, K.-W. Controlling MoO<sub>2</sub> and MoO<sub>3</sub> phases in MoO<sub>x</sub>/CNTs nanocomposites and their application to anode materials for lithium-ion batteries and capacitors. *Electrochim. Acta* **2021**, *388*, 138635. [[CrossRef](#)]
13. Bokhari, S.W.; Siddique, A.H.; Sherrell, P.C.; Yue, X.; Karumbaiah, K.M.; Wei, S.; Ellis, A.V.; Gao, W. Advances in graphene-based supercapacitor electrodes. *Energy Rep.* **2020**, *6*, 2768–2784. [[CrossRef](#)]
14. Kumar, R.; Sahoo, S.; Joanni, E.; Singh, R.K. A review on the current research on microwave processing techniques applied to graphene-based supercapacitor electrodes: An emerging approach beyond conventional heating. *J. Energy Chem.* **2022**, *74*, 252–282. [[CrossRef](#)]
15. Li, Z.; Cai, W.; Liu, J.; Zhou, M.; Cheng, L.; Yu, H.; Song, L.; Gui, Z.; Hu, Y. One-pot exfoliation and synthesis of hydroxyapatite-functionalized graphene as multifunctional nanomaterials based on electrochemical approach. *Compos. Part A Appl. Sci. Manuf.* **2021**, *149*, 106583. [[CrossRef](#)]
16. Huang, Z.; Luo, P.; Zheng, H.; Lyu, Z. Sulfur-doped graphene promoted Li<sub>4</sub>Ti<sub>5</sub>O<sub>12</sub>@C nanocrystals for lithium-ion batteries. *J. Alloys Compd.* **2022**, *908*, 164599. [[CrossRef](#)]
17. Mo, R.; Tan, X.; Li, F.; Tao, R.; Xu, J.; Kong, D.; Wang, Z.; Xu, B.; Wang, X.; Wang, C.; et al. Tin-graphene tubes as anodes for lithium-ion batteries with high volumetric and gravimetric energy densities. *Nat. Commun.* **2020**, *11*, 1374. [[CrossRef](#)]
18. Dong, Y.; Yan, C.; Zhao, H.; Lei, Y. Recent Advances in 2D Heterostructures as Advanced Electrode Materials for Potassium-Ion Batteries. *Small Struct.* **2022**, *3*, 2100221. [[CrossRef](#)]
19. Zhu, J.; Tu, W.; Pan, H.; Zhang, H.; Liu, B.; Cheng, Y.; Deng, Z.; Zhang, H. Self-Templating Synthesis of Hollow Co<sub>3</sub>O<sub>4</sub> Nanoparticles Embedded in N,S-Dual-Doped Reduced Graphene Oxide for Lithium Ion Batteries. *ACS Nano* **2020**, *14*, 5780–5787. [[CrossRef](#)]
20. Gao, C.; Jiang, Z.; Wang, P.; Jensen, L.R.; Zhang, Y.; Yue, Y. Optimized assembling of MOF/SnO<sub>2</sub>/Graphene leads to superior anode for lithium ion batteries. *Nano Energy* **2020**, *74*, 104868. [[CrossRef](#)]
21. Ren, Y.; Xiang, L.; Yin, X.; Xiao, R.; Zuo, P.; Gao, Y.; Yin, G.; Du, C. Ultrathin Si Nanosheets Dispersed in Graphene Matrix Enable Stable Interface and High Rate Capability of Anode for Lithium-ion Batteries. *Adv. Funct. Mater.* **2022**, *32*, 2110046. [[CrossRef](#)]
22. Jing, P.; Liu, K.; Soule, L.; Wang, J.; Li, T.; Zhao, B.; Liu, M. Engineering the architecture and oxygen deficiency of T-Nb<sub>2</sub>O<sub>5</sub>-carbon-graphene composite for high-rate lithium-ion batteries. *Nano Energy* **2021**, *89*, 106398. [[CrossRef](#)]
23. Fan, Z.; Wang, Y.; Zheng, S.; Xu, K.; Wu, J.; Chen, S.; Liang, J.; Shi, A.; Wang, Z. A submicron Si@C core-shell intertwined with carbon nanowires and graphene nanosheet as a high-performance anode material for lithium ion battery. *Energy Storage Mater.* **2021**, *39*, 1–10. [[CrossRef](#)]
24. Xue, H.; Wu, Y.; Zou, Y.; Shen, Y.; Liu, G.; Li, Q.; Yin, D.; Wang, L.; Ming, J. Unraveling Metal Oxide Role in Exfoliating Graphite: New Strategy to Construct High-Performance Graphene-Modified SiO<sub>x</sub>-Based Anode for Lithium-Ion Batteries. *Adv. Funct. Mater.* **2020**, *30*, 1910657. [[CrossRef](#)]
25. Wang, C.; Wang, M.; He, Z.; Liu, L.; Huang, Y. Rechargeable aqueous zinc–manganese dioxide/Graphene batteries with high rate capability and large capacity. *ACS Appl. Energy Mater.* **2020**, *3*, 1742–1748. [[CrossRef](#)]
26. Wang, C.; Zeng, Y.; Xiao, X.; Wu, S.; Zhong, G.; Xu, K.; Wei, Z.; Su, W.; Lu, X. γ-MnO<sub>2</sub> nanorods/graphene composite as efficient cathode for advanced rechargeable aqueous zinc-ion battery. *J. Energy Chem.* **2020**, *43*, 182–187. [[CrossRef](#)]
27. Liu, T.; Yang, Y.; Cao, S.; Xiang, R.; Zhang, L.; Yu, J. Pore Perforation of Graphene Coupled with In Situ Growth of Co<sub>3</sub>Se<sub>4</sub> for High-Performance Na-Ion Battery. *Adv. Mater.* **2023**, *35*, 2207752. [[CrossRef](#)]
28. Dai, C.; Sun, G.; Hu, L.; Xiao, Y.; Zhang, Z.; Qu, L. Recent progress in graphene-based electrodes for flexible batteries. *InfoMat* **2020**, *2*, 509–526. [[CrossRef](#)]
29. Lv, W.; Li, Z.; Deng, Y.; Yang, Q.-H.; Kang, F. Graphene-based materials for electrochemical energy storage devices: Opportunities and challenges. *Energy Storage Mater.* **2016**, *2*, 107–138. [[CrossRef](#)]

30. Khan, B.M.; Oh, W.C.; Nuengmatch, P.; Ullah, K. Role of graphene-based nanocomposites as anode material for Lithium-ion batteries. *Mater. Sci. Eng. B* **2023**, *287*, 116141. [[CrossRef](#)]
31. Ullah, K.; Shah, N.; Wadood, R.; Khan, B.M.; Oh, W.C. Recent trends in graphene based transition metal oxides as anode materials for rechargeable lithium-ion batteries. *Nano Trends* **2023**, *1*, 100004. [[CrossRef](#)]
32. Bonaccorso, F.; Colombo, L.; Yu, G.; Stoller, M.; Tozzini, V.; Ferrari, A.C.; Ruoff, R.S.; Pellegrini, V. Graphene, related two-dimensional crystals, and hybrid systems for energy conversion and storage. *Sci. Adv.* **2015**, *347*, 1246501. [[CrossRef](#)]
33. Rajoba, S.J.; Jadhav, L.D.; Kalubarme, R.S.; Patil, P.S.; Varma, S.; Wani, B. Electrochemical performance of LiFePO<sub>4</sub>/GO composite for Li-ion batteries. *Ceram. Int.* **2018**, *44*, 6886–6893. [[CrossRef](#)]
34. Birkel, C.R.; Roberts, M.R.; McTurk, E.; Bruce, P.G.; Howey, D.A. Degradation diagnostics for lithium ion cells. *J. Power Sources* **2017**, *341*, 373–386. [[CrossRef](#)]
35. Ando, K.; Matsuda, T.; Imamura, D. Degradation diagnosis of lithium-ion batteries with a LiNi<sub>0.5</sub>Co<sub>0.2</sub>Mn<sub>0.3</sub>O<sub>2</sub> and LiMn<sub>2</sub>O<sub>4</sub> blended cathode using dV/dQ curve analysis. *J. Power Sources* **2018**, *390*, 278–285. [[CrossRef](#)]
36. Li, A.G.; West, A.C.; Preindl, M. Towards unified machine learning characterization of lithium-ion battery degradation across multiple levels: A critical review. *Appl. Energy* **2022**, *316*, 119030. [[CrossRef](#)]
37. Xiong, R.; Pan, Y.; Shen, W.; Li, H.; Sun, F. Lithium-ion battery aging mechanisms and diagnosis method for automotive applications: Recent advances and perspectives. *Renew. Sustain. Energy Rev.* **2020**, *131*, 110048. [[CrossRef](#)]
38. Ambrosi, A.; Pumera, M. Exfoliation of layered materials using electrochemistry. *Chem. Soc. Rev.* **2018**, *47*, 7213–7224. [[CrossRef](#)]
39. Tao, P.; Yao, S.; Liu, F.; Wang, B.; Huang, F.; Wang, M. Recent advances in exfoliation techniques of layered and non-layered materials for energy conversion and storage. *J. Mater. Chem. A* **2019**, *7*, 23512–23536. [[CrossRef](#)]
40. Xu, Y.; Cao, H.; Xue, Y.; Li, B.; Cai, W. Liquid-phase exfoliation of graphene: An overview on exfoliation media, techniques, and challenges. *Nanomaterials* **2018**, *8*, 942. [[CrossRef](#)]
41. Duong, D.L.; Yun, S.J.; Lee, Y.H. van der Waals layered materials: Opportunities and challenges. *ACS Nano* **2017**, *11*, 11803–11830. [[CrossRef](#)] [[PubMed](#)]
42. Kamisan, A.I.; Kudin, T.I.T.; Omar, A.F.C.; Taib, M.F.M.; Hassan, O.H.; Ali, A.M.M.; Yahya, M.Z.A. Recent advances on graphene-based materials as cathode materials in lithium-sulfur batteries. *Int. J. Hydrogen Energy* **2022**, *47*, 8630–8657. [[CrossRef](#)]
43. Wu, S.; Xu, R.; Lu, M.; Ge, R.; Iocozzia, J.; Han, C.; Jiang, B.; Lin, Z. Graphene-containing nanomaterials for lithium-ion batteries. *Adv. Energy Mater.* **2015**, *5*, 1500400. [[CrossRef](#)]
44. Lee, S.J.; Theerthagiri, J.; Nithyadharseni, P.; Arunachalam, P.; Balaji, D.; Kumar, A.M.; Madhavan, J.; Mittal, V.; Choi, M.Y. Heteroatom-doped graphene-based materials for sustainable energy applications: A review. *Renew. Sustain. Energy Rev.* **2021**, *143*, 110849. [[CrossRef](#)]
45. Ma, Y.; Han, J.; Wang, M.; Chen, X.; Jia, S. Electrophoretic deposition of graphene-based materials: A review of materials and their applications. *J. Mater.* **2018**, *4*, 108–120. [[CrossRef](#)]
46. Li, G.; Huang, B.; Pan, Z.; Su, X.; Shao, Z.; An, L. Advances in three-dimensional graphene-based materials: Configurations, preparation and application in secondary metal (Li, Na, K, Mg, Al)-ion batteries. *Energy Environ. Sci.* **2019**, *12*, 2030–2053. [[CrossRef](#)]
47. Lu, Y.; Yang, F.; Wang, G.G.; Zhang, T.; Wang, P. Recent development of graphene-based materials for cathode application in lithium batteries: A review and outlook. *Int. J. Electrochem. Sci.* **2019**, *14*, 5961–5971. [[CrossRef](#)]
48. Nguyen, D.C.; Tran, D.T.; Doan, T.L.L.; Kim, D.H.; Kim, N.H.; Lee, J.H. Rational design of core@ shell structured CoS<sub>x</sub>@ Cu<sub>2</sub>MoS<sub>4</sub> hybridized MoS<sub>2</sub>/N, S-codoped graphene as advanced electrocatalyst for water splitting and Zn-air battery. *Adv. Energy Mater.* **2020**, *10*, 1903289. [[CrossRef](#)]
49. Lai, C.; Gong, M.; Zhou, Y.; Fang, J.; Huang, L.; Deng, Z.; Liu, X.; Zhao, T.; Lin, R.; Wang, K. Sulphur modulated Ni<sub>3</sub>FeN supported on N/S co-doped graphene boosts rechargeable/flexible Zn-air battery performance. *Appl. Catal. B Environ.* **2020**, *274*, 119086. [[CrossRef](#)]
50. Lim, J.; Jung, J.-W.; Kim, N.-Y.; Lee, G.Y.; Lee, H.J.; Lee, Y.; Choi, D.S.; Yoon, K.R.; Kim, Y.-H.; Kim, I.-D. N<sub>2</sub>-dopant of graphene with electrochemically switchable bifunctional ORR/OER catalysis for Zn-air battery. *Energy Storage Mater.* **2020**, *32*, 517–524. [[CrossRef](#)]
51. Wang, Y.; Xu, N.; He, R.; Peng, L.; Cai, D.; Qiao, J. Large-scale defect-engineering tailored tri-doped graphene as a metal-free bifunctional catalyst for superior electrocatalytic oxygen reaction in rechargeable Zn-air battery. *Appl. Catal. B Environ.* **2021**, *285*, 119811. [[CrossRef](#)]
52. Shao, G.; Hanaor, D.A.; Wang, J.; Kober, D.; Li, S.; Wang, X.; Shen, X.; Bekheet, M.F.; Gurlo, A. Polymer-derived SiOC integrated with a graphene aerogel as a highly stable Li-ion battery anode. *ACS Appl. Mater. Interfaces* **2020**, *12*, 46045–46056. [[CrossRef](#)] [[PubMed](#)]
53. Chen, H.; Liu, R.; Wu, Y.; Cao, J.; Chen, J.; Hou, Y.; Guo, Y.; Khatoon, R.; Chen, L.; Zhang, Q. Interface coupling 2D/2D SnSe<sub>2</sub>/graphene heterostructure as long-cycle anode for all-climate lithium-ion battery. *Chem. Eng. J.* **2021**, *407*, 126973. [[CrossRef](#)]
54. Tang, Y.; Wang, X.; Chen, J.; Wang, X.; Wang, D.; Mao, Z. PVP-assisted synthesis of g-C<sub>3</sub>N<sub>4</sub>-derived N-doped graphene with tunable interplanar spacing as high-performance lithium/sodium ions battery anodes. *Carbon* **2021**, *174*, 98–109. [[CrossRef](#)]
55. Zhang, X.; Tang, Y.; He, P.; Zhang, Z.; Chen, T. Edge-rich vertical graphene nanosheets templating V<sub>2</sub>O<sub>5</sub> for highly durable zinc ion battery. *Carbon* **2021**, *172*, 207–213. [[CrossRef](#)]

56. Xiang, B.; An, W.-L.; Fu, J.-J.; Mei, S.-X.; Guo, S.-G.; Zhang, X.-M.; Gao, B.; Chu, P.K. Graphene-encapsulated blackberry-like porous silicon nanospheres prepared by modest magnesiothermic reduction for high-performance lithium-ion battery anode. *Rare Met.* **2021**, *40*, 383–392. [[CrossRef](#)]
57. Li, S.; Liu, Y.; Zhao, X.; Shen, Q.; Zhao, W.; Tan, Q.; Zhang, N.; Li, P.; Jiao, L.; Qu, X. Sandwich-like heterostructures of MoS<sub>2</sub>/graphene with enlarged interlayer spacing and enhanced hydrophilicity as high-performance cathodes for aqueous zinc-ion batteries. *Adv. Mater.* **2021**, *33*, 2007480. [[CrossRef](#)]
58. Ma, J.; Kong, Y.; Liu, S.; Li, Y.; Jiang, J.; Zhou, Q.; Huang, Y.; Han, S. Flexible Phosphorus-Doped Graphene/Metal–Organic Framework-Derived Porous Fe<sub>2</sub>O<sub>3</sub> Anode for Lithium-Ion Battery. *ACS Appl. Energy Mater.* **2020**, *3*, 11900–11906. [[CrossRef](#)]
59. Sun, C.; Wang, Y.-J.; Gu, H.; Fan, H.; Yang, G.; Ignaszak, A.; Tang, X.; Liu, D.; Zhang, J. Interfacial coupled design of epitaxial Graphene@SiC Schottky junction with built-in electric field for high-performance anodes of lithium ion batteries. *Nano Energy* **2020**, *77*, 105092. [[CrossRef](#)]
60. Ma, Y.; Qu, H.; Wang, W.; Yu, Y.; Zhang, X.; Li, B.; Wang, L. Si/SiO<sub>2</sub>@Graphene Superstructures for High-Performance Lithium-Ion Batteries. *Adv. Funct. Mater.* **2022**, *33*, 2211648. [[CrossRef](#)]
61. Zhao, Q.; Liu, J.; Li, X.; Xia, Z.; Zhang, Q.; Zhou, M.; Tian, W.; Wang, M.; Hu, H.; Li, Z.; et al. Graphene oxide-induced synthesis of button-shaped amorphous Fe<sub>2</sub>O<sub>3</sub>/rGO/CNFs films as flexible anode for high-performance lithium-ion batteries. *Chem. Eng. J.* **2019**, *369*, 215–222. [[CrossRef](#)]
62. Chen, H.; Ma, X.; Shen, P.K. NiCo<sub>2</sub>S<sub>4</sub> nanocores in-situ encapsulated in graphene sheets as anode materials for lithium-ion batteries. *Chem. Eng. J.* **2019**, *364*, 167–176. [[CrossRef](#)]
63. Dong, X.; Zheng, X.; Deng, Y.; Wang, L.; Hong, H.; Ju, Z. SiO<sub>2</sub>/N-doped graphene aerogel composite anode for lithium-ion batteries. *J. Mater. Sci.* **2020**, *55*, 13023–13035. [[CrossRef](#)]
64. Liu, J.; Khanam, Z.; Ahmed, S.; Wang, T.; Wang, H.; Song, S. Flexible Antifreeze Zn-Ion Hybrid Supercapacitor Based on Gel Electrolyte with Graphene Electrodes. *ACS Appl. Mater. Interfaces* **2021**, *13*, 16454–16468. [[CrossRef](#)] [[PubMed](#)]
65. Wang, F.; Lin, S.; Lu, X.; Hong, R.; Liu, H. Poly-dopamine carbon-coated stable silicon/graphene/CNT composite as anode for lithium ion batteries. *Electrochim. Acta* **2022**, *404*, 139708. [[CrossRef](#)]
66. Rosaiah, P.; Niyitanga, T.; Sambasivam, S.; Kim, H. Graphene based magnetite carbon nanofiber composites as anodes for high-performance Li-ion batteries. *New J. Chem.* **2023**, *47*, 482–490. [[CrossRef](#)]
67. Mu, Y.; Han, M.; Li, J.; Liang, J.; Yu, J. Growing vertical graphene sheets on natural graphite for fast charging lithium-ion batteries. *Carbon* **2021**, *173*, 477–484. [[CrossRef](#)]
68. Xu, S.; Zhou, J.; Wang, J.; Pathirana, S.; Oncel, N.; Robert Ilango, P.; Zhang, X.; Mann, M.; Hou, X. In Situ Synthesis of Graphene-Coated Silicon Monoxide Anodes from Coal-Derived Humic Acid for High-Performance Lithium-Ion Batteries. *Adv. Funct. Mater.* **2021**, *31*, 2101645. [[CrossRef](#)]
69. Dong, Y.; Wu, Z.-S.; Ren, W.; Cheng, H.-M.; Bao, X. Graphene: A promising 2D material for electrochemical energy storage. *Sci. Bull.* **2017**, *62*, 724–740. [[CrossRef](#)]
70. Wang, L.; Hu, X. Recent advances in porous carbon materials for electrochemical energy storage. *Chem. Asian J.* **2018**, *13*, 1518–1529. [[CrossRef](#)]
71. Chen, Z.; Wang, J.; Yu, F.; Zhang, Z.; Gao, X. Preparation and properties of graphene oxide-modified poly(melamine-formaldehyde) microcapsules containing phase change material n-dodecanol for thermal energy storage. *J. Mater. Chem. A* **2015**, *3*, 11624–11630. [[CrossRef](#)]
72. Aadil, M.; Zulfiqar, S.; Sabeeh, H.; Warsi, M.F.; Shahid, M.; Alsafari, I.A.; Shakir, I. Enhanced electrochemical energy storage properties of carbon coated Co<sub>3</sub>O<sub>4</sub> nanoparticles-reduced graphene oxide ternary nano-hybrids. *Ceram. Int.* **2020**, *46*, 17836–17845. [[CrossRef](#)]
73. Wu, H.-Y.; Li, S.-T.; Shao, Y.-W.; Jin, X.-Z.; Qi, X.-D.; Yang, J.-H.; Zhou, Z.-W.; Wang, Y. Melamine foam/reduced graphene oxide supported form-stable phase change materials with simultaneous shape memory property and light-to-thermal energy storage capability. *Chem. Eng. J.* **2020**, *379*, 122373. [[CrossRef](#)]
74. He, D.; Zhang, Y.; Cao, D.; Sun, M.; Xia, J.; Yang, Y.; Ding, Y.; Chen, H. A flexible free-standing FeF<sub>3</sub>/reduced graphene oxide film as cathode for advanced lithium-ion battery. *J. Alloys Compd.* **2022**, *909*, 164702. [[CrossRef](#)]
75. Park, S.; Oh, J.; Kim, J.M.; Guccini, V.; Hwang, T.; Jeon, Y.; Salazar-Alvarez, G.; Piao, Y. Facile preparation of cellulose nanofiber derived carbon and reduced graphene oxide co-supported LiFePO<sub>4</sub> nanocomposite as enhanced cathode material for lithium-ion battery. *Electrochim. Acta* **2020**, *354*, 136707. [[CrossRef](#)]
76. Kang, M.S.; Park, S.K.; Nakhani, P.; Shin, K.H.; Yeon, J.S.; Park, H.S. Mesoporous VO<sub>2</sub>(B) nanorods deposited onto graphene architectures for enhanced rate capability and cycle life of Li ion battery cathodes. *J. Alloys Compd.* **2021**, *855*, 157361. [[CrossRef](#)]
77. Adepoju, A.A.; Doumbia, M.; Williams, Q.L. Graphene Nanoplatelet Additives for High C-rate LiFePO<sub>4</sub> Battery Cathodes. *Jom* **2020**, *72*, 3170–3175. [[CrossRef](#)]
78. Zeng, S.; Xu, Q.; Jin, H.; Zeng, L.; Wang, Y.; Lai, W.; Yao, Q.; Zhang, J.; Chen, Q.; Qian, Q. A green strategy towards fabricating FePO<sub>4</sub>-graphene oxide for high-performance cathode of lithium/sodium-ion batteries recovered from spent batteries. *J. Electroanal. Chem.* **2022**, *913*, 116287. [[CrossRef](#)]
79. Liang, L.; Sun, X.; Zhang, J.; Hou, L.; Sun, J.; Liu, Y.; Wang, S.; Yuan, C. In Situ Synthesis of Hierarchical Core Double-Shell Ti-Doped LiMnPO<sub>4</sub>@NaTi(PO<sub>4</sub>)<sub>2</sub>@C/3D Graphene Cathode with High-Rate Capability and Long Cycle Life for Lithium-Ion Batteries. *Adv. Energy Mater.* **2019**, *9*, 1802847. [[CrossRef](#)]

80. Chen, M.; Zhang, G.; Wu, B.; Liu, M.; Chen, J.; Xiang, W.; Li, W. N-Doped Graphene-Modified Li-Rich Layered Li<sub>1.2</sub>Mn<sub>0.6</sub>Ni<sub>0.2</sub>O<sub>2</sub> Cathode for High-Performance Li-Ion Batteries. *ACS Appl. Energy Mater.* **2022**, *5*, 4307–4317. [[CrossRef](#)]
81. Li, X.; Du, X.; Xu, Y.; Li, J.; Wang, Y.; Meng, Y.; Xiao, D. Three-Dimensional Holey Graphene Enwrapped Li<sub>3</sub>V<sub>2</sub>(PO<sub>4</sub>)<sub>3</sub>/N-Doped Carbon Cathode for High-Rate and Long-Life Li-Ion Batteries. *ChemSusChem* **2022**, *15*, e202201459. [[CrossRef](#)]
82. Chang, U.; Lee, J.T.; Yun, J.M.; Lee, B.; Lee, S.W.; Joh, H.I.; Eom, K.; Fuller, T.F. In Situ Self-Formed Nanosheet MoS<sub>3</sub>/Reduced Graphene Oxide Material Showing Superior Performance as a Lithium-Ion Battery Cathode. *ACS Nano* **2019**, *13*, 1490–1498. [[PubMed](#)]
83. Xu, J.; Yin, Q.; Li, X.; Tan, X.; Liu, Q.; Lu, X.; Cao, B.; Yuan, X.; Li, Y.; Shen, L.; et al. Spheres of Graphene and Carbon Nanotubes Embedding Silicon as Mechanically Resilient Anodes for Lithium-Ion Batteries. *Nano Lett.* **2022**, *22*, 3054–3061. [[CrossRef](#)] [[PubMed](#)]
84. Liu, X.; Jin, Y.; Wang, H.; Yang, X.; Zhang, P.; Wang, K.; Jiang, J. In Situ Growth of Covalent Organic Framework Nanosheets on Graphene as the Cathode for Long-Life High-Capacity Lithium-Ion Batteries. *Adv. Mater.* **2022**, *34*, e2203605. [[CrossRef](#)]
85. Qureshi, Z.A.; Tariq, H.A.; Hafiz, H.M.; Shakoor, R.A.; AlQaradawi, S.; Kahraman, R. Influence of graphene wrapped-cerium oxide coating on spherical LiNi<sub>0.5</sub>Mn<sub>1.5</sub>O<sub>4</sub> particles as cathode in high-voltage lithium-ion batteries. *J. Alloys Compd.* **2022**, *920*, 165989. [[CrossRef](#)]
86. Zhang, Y.; Yuan, X.; Lu, T.; Gong, Z.; Pan, L.; Guo, S. Hydrated vanadium pentoxide/reduced graphene oxide composite cathode material for high-rate lithium ion batteries. *J. Colloid Interface Sci.* **2021**, *585*, 347–354. [[CrossRef](#)] [[PubMed](#)]
87. Chu, J.; Yu, Q.; Han, K.; Xing, L.; Bao, Y.; Wang, W. A novel graphene-wrapped corals-like NiSe<sub>2</sub> for ultrahigh-capacity potassium ion storage. *Carbon* **2020**, *161*, 834–841. [[CrossRef](#)]
88. Chong, S.; Sun, L.; Shu, C.; Guo, S.; Liu, Y.; Wang, W.; Liu, H.K. Chemical bonding boosts nano-rose-like MoS<sub>2</sub> anchored on reduced graphene oxide for superior potassium-ion storage. *Nano Energy* **2019**, *63*, 103868. [[CrossRef](#)]
89. Jia, X.; Zhang, E.; Yu, X.; Lu, B. Facile Synthesis of Copper Sulfide Nanosheet@Graphene Oxide for the Anode of Potassium-Ion Batteries. *Energy Technol.* **2020**, *8*, 1900987. [[CrossRef](#)]
90. Liu, Z.; Wang, J.; Jia, X.; Li, W.; Zhang, Q.; Fan, L.; Ding, H.; Yang, H.; Yu, X.; Li, X.; et al. Graphene Armored with a Crystal Carbon Shell for Ultrahigh-Performance Potassium Ion Batteries and Aluminum Batteries. *ACS Nano* **2019**, *13*, 10631–10642. [[CrossRef](#)]
91. Yao, K.; Xu, Z.; Ma, M.; Li, J.; Lu, F.; Huang, J. Densified Metallic MoS<sub>2</sub>/Graphene Enabling Fast Potassium-Ion Storage with Superior Gravimetric and Volumetric Capacities. *Adv. Funct. Mater.* **2020**, *30*, 2001484. [[CrossRef](#)]
92. Chee, W.K.; Lim, H.N.; Zainal, Z.; Huang, N.M.; Harrison, I.; Andou, Y. Flexible graphene-based supercapacitors: A review. *J. Phys. Chem. C* **2016**, *120*, 4153–4172. [[CrossRef](#)]
93. Lakshmi, K.S.; Vedhanarayanan, B. High-Performance Supercapacitors: A Comprehensive Review on Paradigm Shift of Conventional Energy Storage Devices. *Batter. Supercaps* **2023**, *9*, 202. [[CrossRef](#)]
94. Kumar, R.; del Pino, A.P.; Sahoo, S.; Singh, R.K.; Tan, W.K.; Kar, K.K.; Matsuda, A.; Joanni, E. Laser processing of graphene and related materials for energy storage: State of the art and future prospects. *Prog. Energy Combust. Sci.* **2022**, *91*, 100981. [[CrossRef](#)]
95. Sun, H.-J.; Liu, B.; Peng, T.-J.; Zhao, X.-L. Nitrogen-doped porous 3D graphene with enhanced supercapacitor properties. *J. Mater. Sci.* **2018**, *53*, 13100–13110. [[CrossRef](#)]
96. Yun, Q.; Ge, Y.; Chen, B.; Li, L.; Wa, Q.; Long, H.; Zhang, H. Hybridization of 2D nanomaterials with 3D graphene architectures for electrochemical energy storage and conversion. *Adv. Funct. Mater.* **2022**, *32*, 2202319. [[CrossRef](#)]
97. Khakpour, I.; Baboukani, A.R.; Forouzanfar, S.; Allagui, A.; Wang, C. In-situ exfoliation and integration of vertically aligned graphene for high-frequency response on-chip microsupercapacitors. *J. Power Sources* **2021**, *516*, 230701. [[CrossRef](#)]
98. Salahdin, O.D.; Sayadi, H.; Solanki, R.; Parra, R.M.R.; Al-Thamir, M.; Jalil, A.T.; Izzat, S.E.; Hammid, A.T.; Arenas, L.A.B.; Kianfar, E. Graphene and carbon structures and nanomaterials for energy storage. *Appl. Phys. A* **2022**, *128*, 703. [[CrossRef](#)]
99. He, C.; Qiu, S.; Sun, S.; Zhang, Q.; Lin, G.; Lei, S.; Han, X.; Yang, Y. Electrochemically active phosphotungstic acid assisted prevention of graphene restacking for high-capacitance supercapacitors. *Energy Environ. Mater.* **2018**, *1*, 88–95. [[CrossRef](#)]
100. Goda, E.S.; ur Rehman, A.; Pandit, B.; Al-Shahat Eissa, A.; Eun Hong, S.; Ro Yoon, K. Al-doped Co<sub>9</sub>S<sub>8</sub> encapsulated by nitrogen-doped graphene for solid-state asymmetric supercapacitors. *Chem. Eng. J.* **2022**, *428*, 132470. [[CrossRef](#)]
101. Zhao, Y.; Liu, F.; Zhao, Z.; Bai, P.; Ma, Y.; Alhadhrami, A.; Mersal, G.A.M.; Lin, Z.; Ibrahim, M.M.; El-Bahy, Z.M. Direct ink printing reduced graphene oxide/KCu<sub>7</sub>S<sub>4</sub> electrodes for high-performance supercapacitors. *Adv. Compos. Hybrid Mater.* **2022**, *5*, 1516–1526. [[CrossRef](#)]
102. Thalji, M.R.; Ali, G.A.M.; Liu, P.; Zhong, Y.L.; Chong, K.F. W18O<sub>49</sub> nanowires-graphene nanocomposite for asymmetric supercapacitors employing AlCl<sub>3</sub> aqueous electrolyte. *Chem. Eng. J.* **2021**, *409*, 128216. [[CrossRef](#)]
103. Ansarijad, H.; Shabani-Nooshabadi, M.; Ghoreishi, S.M. Facile synthesis of crumpled-paper like CoWO<sub>4</sub>-CoMn<sub>2</sub>O<sub>4</sub>/N-doped Graphene hybrid nanocomposites for high performance all-solid-state asymmetric supercapacitors. *J. Energy Storage* **2022**, *45*, 103513. [[CrossRef](#)]
104. Huang, A.; El-Kady, M.F.; Chang, X.; Anderson, M.; Lin, C.W.; Turner, C.L.; Kaner, R.B. Facile Fabrication of Multivalent VO<sub>x</sub>/Graphene Nanocomposite Electrodes for High-Energy-Density Symmetric Supercapacitors. *Adv. Energy Mater.* **2021**, *11*, 2100768. [[CrossRef](#)]
105. Kumar, S.; Rehman, M.A.; Lee, S.; Kim, M.; Hong, H.; Park, J.Y.; Seo, Y. Supercapacitors based on Ti(3)C(2)T(x) MXene extracted from supernatant and current collectors passivated by CVD-graphene. *Sci. Rep.* **2021**, *11*, 649. [[CrossRef](#)]

106. Kim, B.-M.; Kim, H.-Y.; Ju, Y.-W.; Shin, J. Influence of the Perovskite  $\text{La}_{0.8}\text{Sr}_{0.2}\text{Mn}_{0.5}\text{Co}_{0.5}\text{O}_{3-\delta}$  on the Electrochemical Performance of the Graphene-Based Supercapacitor. *Energies* **2020**, *13*, 3030. [[CrossRef](#)]
107. Le, Q.B.; Nguyen, T.-H.; Fei, H.; Bubulinca, C.; Munster, L.; Bugarova, N.; Micusik, M.; Kiefer, R.; Dao, T.T.; Omastova, M.; et al. Electrochemical performance of composite electrodes based on rGO, Mn/Cu metal–organic frameworks, and PANI. *Sci. Rep.* **2022**, *12*, 664. [[CrossRef](#)] [[PubMed](#)]
108. Karami, Z.; Youssefi, M.; Raeissi, K.; Zhiani, M. Effect of the morphology of silver layer on electrical conductivity and electrochemical performance of silver/reduced graphene oxide/cotton fabric composite as a flexible supercapacitor electrode. *J. Energy Storage* **2021**, *42*, 103042. [[CrossRef](#)]
109. Haghighi Poudeh, L.; Letofsky-Papst, I.; Cebeci, F.Ç.; Menciloglu, Y.; Yildiz, M.; Saner Okan, B. Facile Synthesis of Single- and Multi-Layer Graphene/Mn<sub>3</sub>O<sub>4</sub> Integrated 3D Urchin-Shaped Hybrid Composite Electrodes by Core-Shell Electrospinning. *ChemNanoMat* **2019**, *5*, 792–801. [[CrossRef](#)]
110. Zhu, Y.Y.; Wang, Y.H.; Wang, Y.T.; Xu, T.J.; Chang, P. Research progress on carbon materials as negative electrodes in sodium-and potassium-ion batteries. *Carbon Energy* **2022**, *4*, 1182–1213. [[CrossRef](#)]
111. Zhang, C.; Pan, H.; Sun, L.; Xu, F.; Ouyang, Y.; Rosei, F. Progress and perspectives of 2D materials as anodes for potassium-ion batteries. *Energy Storage Mater.* **2021**, *38*, 354–378. [[CrossRef](#)]
112. Chen, H.; Guo, F.; Liu, Y.; Huang, T.; Zheng, B.; Ananth, N.; Xu, Z.; Gao, W.; Gao, C. A defect-free principle for advanced graphene cathode of aluminum-ion battery. *Adv. Mater.* **2017**, *29*, 1605958. [[CrossRef](#)] [[PubMed](#)]
113. Kong, Y.; Tang, C.; Huang, X.; Nanjundan, A.K.; Zou, J.; Du, A.; Yu, C. Thermal Reductive Perforation of Graphene Cathode for High-Performance Aluminum-Ion Batteries. *Adv. Funct. Mater.* **2021**, *31*, 2010569. [[CrossRef](#)]
114. Xu, H.; Chen, H.; Gao, C. Advanced graphene materials for sodium/potassium/aluminum-ion batteries. *ACS Mater. Lett.* **2021**, *3*, 1221–1237. [[CrossRef](#)]
115. Childress, A.S.; Parajuli, P.; Zhu, J.; Podila, R.; Rao, A.M. A Raman spectroscopic study of graphene cathodes in high-performance aluminum ion batteries. *Nano Energy* **2017**, *39*, 69–76. [[CrossRef](#)]
116. Zhou, Q.; Zheng, Y.; Wang, D.; Lian, Y.; Ban, C.; Zhao, J.; Zhang, H. Cathode materials in non-aqueous aluminum-ion batteries: Progress and challenges. *Ceram. Int.* **2020**, *46*, 26454–26465. [[CrossRef](#)]

**Disclaimer/Publisher’s Note:** The statements, opinions and data contained in all publications are solely those of the individual author(s) and contributor(s) and not of MDPI and/or the editor(s). MDPI and/or the editor(s) disclaim responsibility for any injury to people or property resulting from any ideas, methods, instructions or products referred to in the content.